

2021

HEPATOPROTECTIVE EFFECTS OF TREPROSTINIL DURING RENAL ISCHEMIA-REPERFUSION INJURY

Joyce Hou
University of Rhode Island, joycehou13@gmail.com

Follow this and additional works at: <https://digitalcommons.uri.edu/theses>

Recommended Citation

Hou, Joyce, "HEPATOPROTECTIVE EFFECTS OF TREPROSTINIL DURING RENAL ISCHEMIA-REPERFUSION INJURY" (2021). *Open Access Master's Theses*. Paper 1997.
<https://digitalcommons.uri.edu/theses/1997>

This Thesis is brought to you for free and open access by DigitalCommons@URI. It has been accepted for inclusion in Open Access Master's Theses by an authorized administrator of DigitalCommons@URI. For more information, please contact digitalcommons-group@uri.edu.

HEPATOPROTECTIVE EFFECTS OF TREPROSTINIL DURING
RENAL ISCHEMIA-REPERFUSION INJURY

BY

JOYCE HOU

A THESIS SUBMITTED IN PARTIAL FULFILLMENT OF THE
REQUIREMENTS FOR THE DEGREE OF

MASTER OF SCIENCE

IN

PHARMACEUTICAL SCIENCES

UNIVERSITY OF RHODE ISLAND

2021

MASTER OF SCIENCE THESIS

OF

JOYCE HOU

APPROVED:

Thesis Committee:

Major Professor Nisanne Ghonem

Ruitang Deng

Gongqin Sun

Brenton DeBoef

DEAN OF THE GRADUATE SCHOOL

UNIVERSITY OF RHODE ISLAND

2021

ABSTRACT

Background: Renal ischemia-reperfusion injury (IRI) occurs during kidney transplantation and causes acute kidney injury as well as liver injury. Renal IRI depletes hepatic antioxidants and leads to hepatic inflammation, tissue damage and hepatic dysfunction through Tlr9 upregulation. There is no treatment available for liver injury during renal IRI. This study examines the hepatoprotective role of treprostnil, a prostacyclin analog, during renal IRI.

Methods: Male Sprague-Dawley rats were divided into four groups: control, sham, IRI-placebo, or IRI-treprostnil and subjected to bilateral ischemia (45 minutes) followed by 1-72 hours of reperfusion. Placebo or treprostnil (100 ng/kg/min) was administered subcutaneously via an osmotic minipump.

Results: Treprostnil significantly reduced peak serum creatinine, BUN, alanine aminotransferase, and aspartate aminotransferase levels vs. IRI-placebo. Treprostnil also restored hepatic antioxidant levels, including superoxide dismutase ($P<0.05$), glutathione ($P<0.01$), catalase ($P<0.001$), and *Gclc* mRNA expression ($P<0.05$), while reducing lipid peroxidation ($P<0.05$) vs. IRI-placebo. Additionally, treatment with treprostnil significantly reduced elevated Tlr9 mRNA and protein *Il-1 β* , *Ccl2*, *Vcam1* and *Serpine1* expression found in the IRI-placebo group. Renal IRI resulted in hepatic apoptosis which was inhibited by treprostnil through reduced hepatic nuclear DNA fragmentation, cytochrome c and cleaved caspase-3 protein expression. Treprostnil enhanced hepatic ATP concentrations and mtDNA copy number while improving mitochondrial dynamics by restoring *Pgc-1a*, significantly upregulating *Mfn1*, *Mfn2*, Sirt3 levels, and reducing renal IRI-induced Drp-1 vs. IRI-placebo. Non-targeted

semi-quantitative proteomics showed improved oxidative stress indices and ATP subunits in the IRI-treprostiniil group vs. IRI-placebo.

Conclusions: Treprostiniil improved hepatic function and antioxidant levels, while suppressing the inflammatory response and alleviating Tlr9-mediated apoptotic injury during renal IRI. Our study provides evidence of treprostiniil's hepatoprotective effect, which supports the therapeutic potential of treprostiniil in reducing hepatic injury during renal IRI.

ACKNOWLEDGMENTS

I would like to acknowledge my major professor Dr. Nisanne Ghonem for providing me the opportunity to join her lab as an undergraduate student. She encouraged me to pursue my graduate studies and I am grateful for the experiences in her lab. Without her guidance and advice, I would not have the laboratory experience, critical thinking skills, nor leadership skills that I have today. Thank you to my committee members, Dr. Ruitang Deng and Dr. Gongqin Sun for their support, encouragement, and contributions to my thesis. Lastly, thank you to Dr. Alison Roberts for chairing my defense.

I would also like to thank my lab mates, colleagues, friends, and family for their support during my journey in graduate school. To my lab mates, past and present, thank you for always being there for me when I needed assistance. To my colleagues, thank you for sharing your expertise and equipment whenever I needed it. To my friends, in and out of school, and my family, thank you for believing in me and my dream of becoming a scientist. I would like to especially thank my mom and dad for the sacrifices they have made in order to provide me with an education so I could be successful academically.

PREFACE

This thesis was written in manuscript style format.

Manuscript: Treprostinil alleviates hepatic oxidative and mitochondrial injury during renal ischemia-reperfusion injury. This manuscript has been prepared for submission to “Biomedicine and Pharmacotherapy.”

TABLE OF CONTENTS

ABSTRACT	ii
ACKNOWLEDGMENTS	iv
PREFACE	v
TABLE OF CONTENTS	vi
MANUSCRIPT – I	1
INTRODUCTION	3
MATERIALS AND METHODS	6
IRI animal model	6
Animal treatment.....	6
Biochemical analysis.....	7
Histological assessment of liver tissue.....	8
TUNEL assay.....	8
Cytosolic and mitochondrial fractionations	8
Liver microsome isolation	9
Western blot analysis	9
Hepatic ATP concentrations	10
mtDNA copy number.....	10
Quantitative real-time PCR analysis (qPCR).....	11
SWATH-MS proteomics analysis.....	11
Statistical analysis.....	12
RESULTS	13
Treprostinil improves renal and hepatic function and reduces hepatic vacuolation	13
Treprostinil alleviates hepatic oxidative stress and lipid peroxidation	14
Treprostinil reduces hepatic TLR9 and inflammation	15
Treprostinil inhibits hepatic apoptosis	16
Treprostinil restores hepatic ATP and ATP synthases.....	17
Treprostinil preserves mitochondrial biogenesis and mtDNA content.....	18
Treprostinil improves hepatic mitochondrial dynamics.....	18
DISCUSSION	20
REFERENCES	33

LIST OF FIGURES

Figure 1. Treprostinil reduces kidney and liver dysfunction.	25
Figure 2. Treprostinil alleviates hepatic oxidative stress levels.....	26
Figure 3. Treprostinil reduces hepatic Tlr9 mRNA and protein expression.	27
Figure 4. Treprostinil reduces hepatic inflammation.	28
Figure 5. Treprostinil inhibits hepatic apoptosis.....	29
Figure 6. Treprostinil restores hepatic ATP and ATP synthase levels.....	30
Figure 7. Treprostinil preserves mitochondrial biogenesis and mtDNA.	31
Figure 8. Treprostinil improves hepatic mitochondrial dynamics after renal IRI.....	32

MANUSCRIPT – I

Prepared for submission to Biomedicine and Pharmacotherapy

Treprostinil alleviates hepatic oxidative and mitochondrial injury during renal ischemia-reperfusion injury

Joyce Hou ^a, Evelyn Tolbert, M.S. ^b, Mark Birkenbach, M.D. ^c, and Nisanne S. Ghonem, Ph.D. ^{a*}

^aDepartment of Biomedical and Pharmaceutical Sciences, College of Pharmacy, University of Rhode Island, 7 Greenhouse Road, Kingston, RI, 02881, USA

^bDivision of Renal Disease, Department of Medicine; ^c Department of Pathology, Rhode Island Hospital, Warren Alpert School of Medicine Brown University, 222 Richmond Street, Providence, RI, 02903, USA

***Corresponding Author:**

Nisanne S. Ghonem
University of Rhode Island
Avedisian Hall 395K
7 Greenhouse Road, Kingston RI, 02881
Office: 401-874-4805
Email: nghonem@uri.edu

Keywords: liver injury, mitochondria, prostacyclin, inflammation, apoptosis

Abbreviations

IRI	Ischemia-reperfusion injury
AKI	Acute kidney injury
SOD	Superoxide dismutase
GSH	Glutathione
CAT	Catalase
ROS	Reactive oxygen species
ATP	Adenosine triphosphate
IL	Interleukin
TLR	Toll-like receptor
mtDNA	Mitochondrial DNA
Mfn	Mitofusin
Pgc-1 α	Peroxisome proliferator-activated receptor gamma coactivator 1 alpha
Drp-1	Dynamin-related protein 1
PGI ₂	Prostacyclin
ALT	Alanine aminotransferase
AST	Aspartate aminotransferase
SCr	Serum creatinine
BUN	Blood urea nitrogen
MDA	Malondialdehyde
H&E	Hematoxylin & eosin
TUNEL	Terminal deoxynucleotidyl transferase dUTP nick end labeling
Sirt3	NAD-dependent deacetylase sirtuin-3
Gapdh	Glyceraldehyde 3-phosphate dehydrogenase
Cox-IV	Cytochrome c oxidase subunit 4
mt-Nd1	mitochondrial encoded NADH-ubiquinone oxidoreductase chain 1
Vcam1	Vascular cell adhesion molecule 1
Serpine1	Serine protease inhibitor, family E, member 1
Gclc	Glutamate-cysteine ligase catalytic subunit
Ccl2	Chemokine ligand 2
18S	18S ribosomal RNA
SWATH-MS	Sequential windowed acquisition of all theoretical fragment ion mass spectra
Gpx	Glutathione peroxidase
Gsta2	Glutathione S-transferase alpha 2
Gstm4	Glutathione S-transferase mu 4

INTRODUCTION

Renal ischemia-reperfusion injury (IRI) is a major cause of morbidity and mortality in several clinical settings, and it is unavoidable during kidney transplantation [1]. Renal IRI leads to acute kidney injury (AKI) [1], requiring subsequent retransplantation and further depleting the existing scarce donor pool. During renal IRI, the blood supply to the kidneys is temporarily restricted (ischemia) then subsequently restored by reoxygenation (reperfusion), which rescues the oxygen deprivation but also exacerbates the ischemic-induced organ injury. Not only are the kidneys damaged, but vital organs, particularly the liver [2], are also damaged as a complication of renal IRI. Consequences of renal IRI-induced hepatic injury include multi-organ injury and increased mortality due to complications of AKI and liver dysfunction [3].

The liver contains an abundance of antioxidants and renal IRI decreases hepatic antioxidant levels, particularly superoxide dismutase (SOD) [4], glutathione (GSH) [5, 6], and catalase (CAT) [7]. Oxidative stress is one of the major mechanisms that contributes to renal IRI-induced hepatic injury [5]. In fact, a weakened antioxidant defense system damages the mitochondria and causes mitochondrial dysfunction through uncontrolled reactive oxygen species (ROS) [8]. Mitochondrial dysfunction increases mitochondrial fission, depletes adenosine triphosphate (ATP), and increases the permeability of the mitochondrial membrane [8], all of which trigger the cytosolic release of cytochrome c and subsequent activation of caspases, resulting in mitochondrial-mediated apoptosis [9]. During renal IRI, pro-apoptotic markers in the liver, e.g., caspase-3, are activated [10] and contribute to liver cell death.

Renal IRI-induced hepatic injury also leads to hepatic inflammation [11]. In particular, toll-like receptor (TLR)-9, which is located intracellularly in endosomes, recognizes pathogen- or damage-associated molecular patterns (DAMP), and triggers the inflammatory response [12]. During renal IRI, hepatic Tlr9 is upregulated by released mitochondrial DNA (mtDNA) [13], a type of DAMP, which leads to the production of pro-inflammatory cytokines, including interleukins (IL), e.g. IL-1 β [14]. The network of mitochondrial proteins that regulate mtDNA maintenance include fusion proteins, e.g., Mitofusin (Mfn) -1, Mfn-2, and Pgc-1 α , along with the fission protein, dynamin-related protein-1 (Drp-1) [15]. Fragmentation of the mitochondria driven by Drp-1 causes mtDNA leakage, resulting in cytosolic mtDNA stress [16]. During renal IRI, mitochondrial fusion proteins are downregulated, while the mitochondrial fission protein is upregulated, resulting in disrupted mitochondrial dynamics [17]. The interaction between mtDNA and Tlr9 can activate neutrophil secretion [18], which further contributes to inflammation in the liver [19] and subsequent hepatic injury.

Thus, a treatment to reduce renal IRI is needed to reduce hepatic oxidative stress and mitochondrial-mediated apoptosis, thereby, reduce the inflammatory response and liver cell death. Currently, however, there are no available therapies to reduce renal IRI-induced liver damage. Prostacyclin (PGI₂) is an endogenous compound with vasodilatory, anti-coagulant, and anti-inflammatory effects [20]. Treprostinil (Remodulin®) is a PGI₂ analog with potent vasodilatory and anti-platelet aggregation properties [21] and FDA-approved for the treatment of pulmonary arterial hypertension. Importantly, treprostinil alleviates IRI during rat AKI [22] and

orthotopic liver transplantation [23]. This study investigates the hepatoprotective effects of treprostinil during renal IRI.

MATERIALS AND METHODS

IRI animal model

Adult male Sprague Dawley rats weighing 200-250 gm (Charles River Laboratories, Wilmington, MA), approximately 7-8 weeks old were housed in a laminar-flow, specific pathogen-free atmosphere in the Central Research Facilities of Rhode Island Hospital (RIH, Providence, RI) with a standard diet and water supplied ad libitum. Animals were randomly divided into four groups: control, sham, IRI-placebo, and IRI-treprostinil. Briefly, animals were anesthetized with isoflurane and subjected to bilateral renal ischemia for 45 minutes, afterward clamps were removed to allow reperfusion for 1-72 hours. Control animals were not subjected to any surgical manipulation and serve as the baseline, whereas sham animals had incisions only, to account for any influence from basic surgical handling or anesthesia. All surgical procedures were performed by the same surgeon who was blinded to treatment. All procedures involving animals were performed with approval from RIH Institutional Animal Care and Use Committee in accordance with the NIH Guide for the Care and Use of Laboratory Animals.

Animal treatment

Treprostinil (Remodulin®) or placebo (sodium chloride, metacresol, sodium citrate, water for injection, United Therapeutics, Corp., Durham, NC, USA) were administered subcutaneously (100 ng/kg/min) via osmotic minipumps (Alzet Inc., Cupertino, CA) and implanted at 18-24 hours before renal IRI to ensure steady-state concentrations at the time of renal IRI. Post-reperfusion, animals were kept under a

heating lamp for 2 hours and were given regular food and water ad libitum. The general condition of the rats was checked three times daily and animals were euthanized by inhalation of carbon dioxide followed by cervical dislocation if needed. Blood and liver tissue were collected at 1-72 hours post-reperfusion, and liver tissue was formalin-fixed or snap-frozen then stored at -80 °C for analysis.

Biochemical analysis

Serum alanine aminotransferase (ALT) and aspartate aminotransferase (AST) activity levels were determined using the Infinity ALT and AST assays (Thermo Fisher Scientific, Waltham, MA). Serum creatinine (SCr) and blood urea nitrogen (BUN) levels were measured by biochemical assay (Bioassay Systems, Hayward, CA), n=3-10/group. The hepatic activity of SOD, GSH, and CAT were determined using biochemical assay (Cayman Chemical, Ann Arbor, MI). Tissue samples were homogenized, and protein quantification was calculated using bovine serum albumin (Thermo Fisher Scientific) as a standard prior to SOD, GSH, and CAT determination. Hepatic lipid peroxidation was measured by malondialdehyde (MDA) in liver homogenate using a fluorometric thiobarbituric acid reactive substance (TBARS) assay (BioAssay Systems) per manufacturer instructions (n = 3-6/group). Fluorescence ($\lambda_{\text{ex/em}}$ 530/550 nm) was measured using a SpectraMax iD3 microplate reader (Molecular Devices, San Jose, CA).

Histological assessment of liver tissue

Liver tissue was isolated, fixed in 10% formalin and embedded in paraffin. Sections were cut at 4 μm , stained with hematoxylin and eosin (H&E) and evaluated by a pathologist under light microscopy in a blinded fashion.

TUNEL assay

Paraffin-embedded liver tissue sections (5 μm) were used to perform Click-iT™ Plus TUNEL Assay (Alexa Fluor™ 647 dye, Invitrogen, Carlsbad, CA). Nuclei were counterstained with Hoechst dye (Invitrogen) according to manufacturer's instruction. Liver sections were viewed under a Nikon Eclipse Ti2 inverted confocal microscope (Nikon, Tokyo, Japan). Random fields (n = 3-5/section) with the same acquisition setting were imaged per slide (n = 3-4/group). Hepatic DNA fragmentation was semi-quantitated based on the intensity ratio of TUNEL and Hoechst using Image J ($\times 200$, scale bar = 100 μm).

Cytosolic and mitochondrial fractionations

Snap-frozen liver tissue was homogenized in 0.25 M sucrose buffer (Millipore Sigma, Burlington, MA), 0.1 mM EDTA (Bio-Rad, Hercules, CA), 10 mM HEPES (Fisher Scientific, Hampton, NH) with protease and phosphatase inhibitor (Thermo Fisher Scientific) using a Dounce homogenizer. Supernatant was collected and centrifuged at 13,000 $\times g$ for 15 mins and collected as the cytosolic fraction. The crude mitochondria pellet was washed twice and suspended in PBS containing protease and phosphatase inhibitor cocktail (Thermo Fisher Scientific) and 0.1% Triton X-100, then disrupted

twice with a sonicator at 40% of maximum setting for 10 seconds. Following lysate centrifugation, supernatant was collected as the mitochondria fraction.

Liver microsome isolation

Microsomes were isolated from rat liver tissue using a differential centrifugation procedure as described by XenoTech (Sekisui XenoTech, Kansas City, KS). Briefly, tissue was homogenized in a buffer containing 0.25 M sucrose, 50 mM Tris-HCl (pH 7.4), 2 mM EDTA, 150 mM potassium chloride, using a Bead Ruptor 24 (Omni International, Kennesaw, GA), then centrifuged at 10,000 x g for 20 minutes (4 °C). The supernatant was centrifuged at 100,000 x g for 65 minutes (4 °C), and then the microsomal pellet was resuspended in a medium consisting of 0.25 M sucrose using a Dounce homogenizer.

Western blot analysis

Total, cytosolic, mitochondrial, and microsomal liver protein fractions were separated by electrophoresis using polyacrylamide gels and transferred to PVDF membranes. Membranes were incubated overnight at 4 °C with antibodies for caspase-3 (Cat# 14220), Drp-1 (Cat# 8570, Cell Signaling Technology, Danvers, MA), cytochrome C (Cat# sc-13156), Sirt3 (Cat# sc-365175), Tlr9 (Cat# sc-52966), β -actin (Cat# sc-47778), Gapdh (Cat# sc-32233) or Cox-IV (Cat# sc-517553, Santa Cruz Biotechnology, Dallas, TX), followed by IRDye® donkey anti-rabbit or goat anti-mouse IgG (H+L) 680 RD and goat anti-mouse IRDye® 800 CW applied at room temperature for 1 hour. Blots were imaged using LI-COR Odyssey® Clx scanner (Li-

Cor Biosciences, Lincoln, NE). Protein band density was determined using Image J, normalized to β -actin (whole lysate), Gapdh (cytosol, microsomal), or Cox-IV (mitochondria) protein levels, and expressed as fold-change vs. sham animals (n = 3-5/group). Protein concentrations were measured using a Pierce™ BCA Protein Assay Kit (Thermo Fisher Scientific).

Hepatic ATP concentrations

Snap-frozen liver tissue was homogenized in ice-cold 2% trichloroacetic acid. The supernatants were collected and neutralized with Tris-acetate (100 mM) and EDTA (2 mM, pH, 7.8) (n = 4-6/group). ATP concentrations were determined using the Enliten ATP Assay System Bioluminescence Detection Kit (Promega, Madison, WI).

Hepatic mtDNA copy number

DNA was extracted from snap-frozen liver tissue (n=4-5/group) using the DNeasy Blood and Tissue Kit (Qiagen, Hilden, Germany). DNA concentration was determined using a Nanodrop One^C (Thermo Fisher Scientific). Mitochondrial DNA (mtDNA) and nuclear DNA (nDNA) content were determined by mitochondrial encoded NADH-ubiquinone oxidoreductase chain 1 (mt-*Nd1*) and nuclear DNA (*18S*) using Taqman[®] probes (Applied Biosystems, Foster City, CA), respectively. Quantitative real-time PCR was performed using a ViiA 7 Real-Time PCR System (Life Technologies, Carlsbad, CA). The hepatic mtDNA copy number was calculated using the ratio between mitochondrial and nuclear DNA (mtDNA/nDNA) [24].

Quantitative real-time PCR analysis (qPCR)

RNA was extracted from snap-frozen liver sections using TRIzol™ (Invitrogen) according to manufacturer's protocol. The purity and concentration of RNA were measured at 260/280 nm by Nanodrop (Thermo Fisher Scientific). Two micrograms of total RNA were used to generate cDNA using SuperScript™ IV First-Strand Synthesis System kit (Invitrogen). Hepatic mRNA levels of *Gclc*, *Tlr9*, *Il-1β*, *Ccl2*, *Vcam1*, *Serpine1*, *Mfn1*, *Mfn2*, *Pgc-1α*, and *18s* were analyzed using Taqman® probes (Applied Biosystems). Relative mRNA expression was calculated using the $\Delta\Delta C_t$ method and normalized to *18S* expression (n = 4-5/group). Real-time qPCR was performed using a ViiA 7 Real-Time PCR System (Life Technologies).

SWATH-MS proteomics analysis

The effects of liver injury during renal IRI ± treprostinil treatment on the hepatic proteome was assessed using sequential window acquisition of all theoretical mass spectra (SWATH-LC/MS/MS). Snap frozen rat liver tissue were weighed on ice, placed in bead-mill tubes, and homogenized in a urea buffer (8 M urea, 50 mM triethylammonium bicarbonate, 10 mM dithiothreitol, and protease inhibitor cocktail (Thermo Fisher Scientific) using a Bead Ruptor 24 (Omni International), then centrifuged at 12,000 x g (4°C) and the supernatant was collected. Protein concentration was measured using a Pierce™ BCA Protein Assay Kit. The samples were diluted to 500 µg/100 µl before digestion. Proteins were digested with TPCK-treated trypsin (AB SCIEX, Framingham, MA) at trypsin/protein ratio of 1:20 under high pressure cycles in a Barocycler NEP2320 (Pressure BioSciences, South Easton,

MA. The reaction was stopped by the addition of water:acetonitrile (50:50) with 5% formic acid. The supernatant containing peptides was collected for mass spectrometry analysis [25]. The samples were analyzed using a SCIEX 5600 TripleTOF mass spectrometer coupled to an Acquity UHPLC HClass System (Waters Corp., Milford, MA) [25]. Afterwards, proteins were identified, and relative quantification was performed through SWATH-MS acquisition, followed by data-dependent analysis using Spectronaut™ software (Biognosys AG, Schlieren, Switzerland).

Statistical analysis

All data are represented as the mean \pm standard error of the mean (SEM). One- or two-way ANOVA followed by Tukey-multiple comparisons test was used to determine the differences between groups. Statistical significance was set at $P < 0.05$. GraphPad Prism 8.3.0 (GraphPad Software, Inc., La Jolla, CA) was used for statistical analysis and graphing.

RESULTS

Treprostinil improves renal and hepatic function

Renal IRI was demonstrated by measuring SCr and BUN levels, two classical markers of kidney injury. In IRI-placebo animals, SCr and BUN levels were significantly elevated and reached peak levels at 24-hr post-reperfusion vs. sham (1.8 ± 0.3 mg/dL vs. 0.6 ± 0.06 mg/dL and 151 ± 20.4 mg/dL vs. 32.5 ± 1.7 mg/dL, respectively, $P < 0.001$). Treatment with treprostinil significantly reduced peak SCr (0.6 ± 0.06 mg/dL) and BUN (74 ± 12.8 mg/dL) vs. IRI-placebo ($P < 0.001$), **Figure 1A and 1B**.

Renal IRI-induced hepatic injury was evaluated by measuring serum ALT and AST levels, which are biomarkers for liver dysfunction. Serum ALT and AST activity were significantly elevated in IRI-placebo animals and reached peak levels at 6-hr post-reperfusion vs. sham (110 ± 6.9 U/L vs. 29 ± 1.6 U/L and 32 ± 3.6 U/L vs. 19 ± 0.6 U/L, respectively, $P < 0.001$). In contrast, treatment with treprostinil significantly reduced peak liver injury with ALT and AST activity at 6-hr post-reperfusion vs. placebo (33 ± 6.6 U/L and 20 ± 1.8 U/L, respectively, $P < 0.001$), **Figure 1C and 1D**.

These results demonstrate that treprostinil improves liver function during renal IRI.

Livers from sham-operated, IRI-placebo and -treprostinil-treated animals were surgically removed at sacrifice, fixed in formalin and embedded in paraffin. Sections stained with hematoxylin and eosin (H&E) were examined under light microscopy by a pathologist blinded as to the treatment group from which each specimen was derived, **Figure 1E**. Light microscopic examination revealed focal coarse cytoplasmic vacuolation of hepatocytes, indicating acute cellular injury in livers from IRI-placebo animals. Injured hepatocytes were consistently localized specifically within peripheral

areas of hepatic lobules, corresponding to hepatic acinus zone 1. In contrast, only minimal vacuolation was noted in hepatocytes from animals pretreated with treprostiniil. No cytoplasmic vacuolation was observed in sham-operated animals.

Treprostiniil alleviates hepatic oxidative stress and lipid peroxidation

We next studied the role of treprostiniil in regulating hepatic oxidative stress during renal IRI. Hepatic SOD activity in IRI-placebo animals significantly decreased at 1-hr post-reperfusion vs. sham animals (29 ± 3.5 vs. 45 ± 3.8 U/mg protein, $P < 0.05$), which treprostiniil restored (44 ± 3.2 U/mg protein, $P < 0.05$ vs. IRI-placebo), **Figure 2A**.

Total hepatic GSH concentrations in IRI-placebo group significantly decreased at 6-hr post-reperfusion compared to sham (626 ± 123 vs. $1,057 \pm 72$ μM /mg protein, respectively, $P < 0.05$). Treatment with treprostiniil significantly improved total GSH content in the liver compared to placebo ($1,130 \pm 59$ vs. 626 ± 123 μM /mg protein, $P < 0.01$), **Figure 2B**. Similarly, hepatic CAT activity in IRI-placebo group significantly decreased compared to sham at 24-hr post-reperfusion ($1,574 \pm 126$ vs. $2,195 \pm 80$ U/mg protein, $P < 0.01$), which treprostiniil also significantly improved ($2,441 \pm 116$, $P < 0.001$ vs. IRI-placebo), **Figure 2C**. Lipid peroxidation promotes the generation of toxic aldehydes, including MDA. The hepatic MDA concentration increased by 1.6-fold in the IRI-placebo group compared to control at 48-hr post-reperfusion (0.6 ± 0.07 vs. 0.36 ± 0.01 μM /mg protein, respectively, $P = 0.09$). On the other hand, treprostiniil significantly reduced hepatic MDA concentrations by 50% relative to IRI-placebo animals (0.3 ± 0.05 vs. 0.6 ± 0.07 μM /mg protein, $P < 0.05$), which nearly restored levels to baseline, **Figure 2D**.

To further investigate the role of treprostiniil in restoring hepatic antioxidants during renal IRI, SWATH-MS-based proteomic analysis was performed. In agreement with our biochemical data, hepatic antioxidants, particularly glutathione synthetase subunits, e.g., Gpx1, Gpx3, Gsta2, Gstm4, Sod2, Cat, and Gclc, were all significantly reduced in IRI-placebo at 24-hr post-reperfusion vs. healthy control ($P < 0.05$), all of which treprostiniil upregulated, **Figure 2E**. In addition, hepatic *Gclc* mRNA expression decreased in the IRI-placebo group by 30% relative to sham at 48-hr post-reperfusion, whereas treatment with treprostiniil upregulated *Gclc* expression by 2.0 ± 0.6 -fold, relative to sham, **Figure 2F**. Taken together, these results demonstrate that renal IRI reduced hepatic antioxidant levels and that treprostiniil alleviates hepatic oxidative stress induced by renal IRI.

Treprostiniil reduces hepatic TLR9 and inflammation

TLR9 is upregulated in the liver during severe renal IRI and activation of TLR9 by mtDNA released from damaged mitochondria contributes to inflammation [13]. In this study, hepatic Tlr9 mRNA and protein expression increased in IRI-placebo animals by 30% and 37% ($P < 0.05$) vs. sham, respectively, highlighting the role of Tlr9-mediated hepatic injury during renal IRI, **Figure 3A, 3B**. A striking contrast was observed in the IRI-treprostiniil group, where Tlr9 mRNA and protein expression were significantly reduced by 61% ($P < 0.05$) and 70% ($P < 0.001$) vs. IRI-placebo, respectively.

Proinflammatory cytokines and adhesion molecules play an important role in the pathophysiology of liver injury during renal IRI [26]. Specifically, *Il-1 β* mRNA expression significantly increased in the IRI-placebo group at 6-hr post-reperfusion by

1.6 ± 0.5-fold relative to sham (P<0.05), **Figure 4A**. Pre-treatment with treprostini decreased *Il-1β* expression by 22% compared to placebo. *Ccl2* expression significantly increased in the IRI-placebo group 24-hr post-reperfusion by 3.4 ± 1.5-fold relative to sham (P<0.05), **Figure 4B**. Subsequently, treprostini significantly reduced *Ccl2* expression by 76% compared to placebo (P<0.05). Vcam1 and Serpin E1 recruit neutrophils to injured tissue to further promote inflammation [27, 28]. In our study, hepatic mRNA *Vcam1* levels were increased in the IRI-placebo group by 1.4 ± 0.2-fold relative to sham (P=0.06) at 24-hr post-reperfusion, whereas pretreatment with treprostini significantly reduced *Vcam1* mRNA expression by 30% vs. IRI-placebo (P<0.05), **Figure 4C**. In IRI-placebo, *Serpine1* mRNA expression was significantly increased by 2.9 ± 1.4-fold relative to sham (P<0.05), which treprostini reduced by 54% compared to placebo (P<0.05), **Figure 4D**. These results support the anti-inflammatory role of treprostini during renal IRI and the reduction in Tlr9 expression suggests that hepatic injury decreases by suppressing the inflammatory response.

Treprostini inhibits hepatic apoptosis

Liver injury due to renal IRI causes mitochondrial dysfunction which leads to hepatic apoptosis [29]. Hepatocyte apoptosis was evaluated by TUNEL staining, as an indicator of DNA fragmentation. In the IRI-placebo group, TUNEL-positive cells were significantly increased by 40% vs. sham (P<0.05) at 6-hr post-reperfusion. In contrast, treprostini significantly reduced DNA fragmentation to nearly that of sham, reflecting a 30% reduction in IRI-induced apoptosis vs. IRI-placebo (P<0.05), **Figure 5A**.

Mitochondria fragmentation releases cytochrome c into the cytosol, which initiates caspase activation [9]. We found that the cytosolic protein expression of hepatic cytochrome c increased in the IRI-placebo group by 1.7 ± 0.2 -fold vs. sham at 3-hr post-reperfusion, which treprostiniil decreased by 24% compared to IRI-placebo, **Figure 5B**. Subsequent activation of caspase-3 by cleavage from procaspase-3 triggers the apoptotic cascade [9]. Here, cleaved caspase-3 protein expression was significantly increased in the IRI-placebo group by 12.4 ± 4.5 -fold at 48-hr post-reperfusion, compared to sham ($P < 0.01$), **Figure 5C**. On the other hand, treprostiniil reduced the cleavage of caspase-3 by 80% compared to placebo ($P < 0.01$). These results suggest that treprostiniil inhibits hepatic apoptosis by suppressing the release of mitochondrial cytochrome c and caspase-3 activation.

Treprostiniil restores hepatic ATP and ATP synthases

ATP is required to maintain mitochondrial homeostasis and disrupted ATP production contributes to dysfunctional mitochondria [30]. In our study, hepatic ATP levels were reduced in the IRI-placebo group by more than 50% of sham levels at 6-hr post-reperfusion, **Figure 6A**. In line with this finding, hepatic proteomic analysis revealed that the ATP synthase subunits 5f1c, 5f1d, 5i ($P < 0.001$), 5j2 ($P < 0.01$), 5l ($P < 0.001$), and 5o ($P < 0.05$) were markedly downregulated in IRI-placebo, compared to control at 24-hr post-reperfusion, **Figure 6B**. In contrast, treprostiniil attenuated the loss of hepatic ATP levels which corresponded with upregulated hepatic ATP synthase subunits. Together, these results demonstrate treprostiniil restores ATP production, which is necessary to maintain mitochondrial function.

Treprostiniil preserves mitochondrial biogenesis and mtDNA content

Mitochondrial biogenesis is an important biological process and necessary for liver recovery and generation after acute injury [31]. The peroxisome proliferator-activated receptor gamma coactivator-1 α (PGC-1 α) is considered one of the master regulators of mitochondrial biogenesis [32]. In this study, hepatic mRNA expression of *Pgc-1 α* was significantly decreased in IRI-placebo group to nearly 50% of sham levels at 24-hr post-reperfusion (P<0.05). Conversely, treprostiniil upregulated *Pgc-1 α* mRNA expression by 1.9-fold (P<0.01 vs. IRI-placebo), which restored mRNA expression to that of sham levels, **Figure 7A**.

Pgc-1 α also regulates mitochondrial DNA copy number [33], which is released into the circulation following renal IRI and activates hepatic TLR9 [13]. Here, we demonstrated that hepatic mtDNA copy number significantly decreased 6-hr post-reperfusion in IRI-placebo group to 70% of sham (P<0.05), which was nearly restored by treprostiniil to sham levels, **Figure 7B**. These findings suggest that a greater amount of hepatic mtDNA content is released into the circulation during renal IRI, which in turn activates Tlr9. In contrast, treprostiniil preserves hepatic mtDNA, likely mediated by the upregulation of hepatic *Pgc-1 α* .

Treprostiniil improves hepatic mitochondrial dynamics

To further investigate the role of treprostiniil in alleviating hepatic mitochondrial injury during renal IRI, we studied hepatic mitochondrial dynamics. Mitochondrial homeostasis is maintained through continuous cycles of fission and fusion and injury

to the liver during renal IRI disrupts this balance of mitochondrial dynamics [29]. We found that the facilitators of outer mitochondrial membrane fusion, Mfn-1 and -2 [31], were compromised in the liver following renal IRI. Specifically, hepatic mRNA expression of *Mfn1* and *Mfn2* decreased in IRI-placebo group by 30% (P=0.08) and 18% relative to sham, respectively, at 24-hr post-reperfusion, **Figure 8A, 8B**. In contrast, treprostiniil upregulated *Mfn1* and *Mfn2* expression by 30% (P<0.01) and 40% (P=0.08), respectively, in comparison to sham.

Following stimulus, such as cellular stress due to renal IRI, the mitochondrial fission protein Drp-1 translocates to the outer mitochondrial membrane where it causes mitochondrial fragmentation [34]. Early post-reperfusion, mitochondrial protein levels of hepatic Drp-1 in IRI-placebo animals significantly increased by 1.8 ± 0.2 -fold vs. sham animals (P<0.01), which treprostiniil significantly decreased (P<0.01) and returned to baseline, **Figure 8C**. Notably, NAD-dependent deacetylase sirtuin-3 (Sirt3), the master regulator of mitochondrial fusion, significantly decreased in IRI-placebo animals by 44% vs. sham (P<0.05) at 6-hr post-reperfusion, **Figure 8C**, which treprostiniil also restored to healthy levels (P<0.01 vs. IRI-placebo). Together, these data demonstrate that treprostiniil improves mitochondrial dynamics by mitigating Drp-1-mediated mitochondrial fission while favorably contributing to Sirt3-mediated mitochondrial fusion.

DISCUSSION

Renal IRI occurs during several clinical situations, including kidney transplantation, and results in kidney injury as well as liver injury [11, 35]. In fact, a correlation between the severity of renal IRI and the severity of liver injury and cell death has been found [11], further supporting the evidence of hepatic damage during renal IRI. Left untreated, hepatic injury during renal IRI can lead to a comorbidity which elevates the risk of mortality [3]. Prostacyclin analogs, including treprostinil (Remodulin®), have been studied for their efficacy in reducing IRI, particularly during liver transplantation [36, 37] and, more recently, during acute kidney injury [22]. Therefore, we hypothesized that treprostinil would protect the liver against injury during renal IRI. This study demonstrates a novel mechanism by which treprostinil improves hepatic function, reduces hepatic oxidative stress, inflammation, mitochondrial damage, and apoptosis during renal IRI.

The liver is highly susceptible to renal damage as a result of IRI during AKI [11, 38]. Animal studies have shown elevated serum ALT and AST levels during renal IRI [2, 7, 10, 39], supporting secondary liver dysfunction. Prostacyclin analogs are effective in reducing liver dysfunction during hepatic IRI, including mice preconditioned with beraprost [40] when subjected to hepatic IRI or pretreated with treprostinil before rat [36] and clinical orthotopic liver transplantation [37]. Treprostinil is a stable PGI₂ analog at room temperature with potent vasodilatory and anti-platelet properties [21] and a half-life of 3-4 hours [41], whereas beraprost is not FDA-approved.

Antioxidants are responsible for protecting the liver from oxidative damage and their depletion serves as a key indicator of the generation of oxygen radicals during renal IRI [42]. Consistent with previous animal studies [5, 7, 11], our results demonstrate that hepatic oxidative injury occurs during renal IRI *in vivo*. We confirmed hepatic oxidative injury through biochemical analyses, particularly the reduced activity levels of SOD, CAT, and GSH, in addition to increased MDA levels. Reduced *Gclc* mRNA expressions patterns also confirmed oxidative injury. Furthermore, proteomic analyses showed that treprostinil restored the depleted antioxidants through increased expression patterns of Gpx1, Gpx3, Gsta2, Gstm4, Sod2, Cat, and Gclc. These data provide further support that PGI₂ restores the oxidant status during hepatic IRI.

Toll-like receptors play a major role in regulating the innate immune system's response to pathogen- or DAMP [12]. Specifically, activation of TLR9 by mtDNA released from apoptotic cells [43] initiates a signaling cascade involving nuclear factor kappa B (NF- κ B) which upregulates proinflammatory cytokines, including Il-1 β [14]. Tlr9 mediates hepatic inflammation by increasing proinflammatory cytokines e.g., Il-6, Ccl2, and Tnf- α [44]. Additionally, Bakker et al. [13] showed that hepatic Tlr9 was selectively upregulated at 24-hr post-reperfusion during renal IRI, further supporting our hypothesis that Tlr9 mediates hepatic injury during renal IRI. Our results show that treprostinil suppresses the mRNA expression of *Il-1 β* and *Ccl2* early post-reperfusion. Overexpression of hepatic adhesions molecules, e.g., Vcam1, Icam1, E- and P-selectin have also been found to increase following renal [26, 39] and hepatic IRI [45], which promote neutrophil-mediated organ injury and contribute to

inflammation [46]. Volpes et al. [28] demonstrated that VCAM1 is highly expressed in the inflamed liver and *Serpine1* is involved in inflammation [47]. In agreement with these findings, our study shows remarkable elevations of hepatic *Vcam1* and *Serpine1* mRNA expressions in IRI-placebo animals, which treprostinil reduces to alleviate hepatic inflammation. In addition, our findings also show that treprostinil suppresses the elevated hepatic *Tlr9* expression, supporting our hypothesis of Tlr9-mediated hepatic inflammation during renal IRI.

Some PGI₂ analogs are ligands for the peroxisome proliferator-activated receptor (PPAR)-alpha [48], a nuclear transcription factor that is predominantly expressed in the liver. In a mouse model of drug-induced liver injury, Fan et al. [49] demonstrated that hepatic Tlr9 protein expression is increased while Ppar- α is downregulated. Interestingly, treprostinil has been shown to activate PPAR- β [50], which downregulates NF- κ B-induced expression of IL-1 β [51, 52] and it also reduces ROS generation [52]. Crosstalk between some PPAR isoforms and TLRs have been studied since they both regulate the inflammatory NF- κ B signaling cascade [53], but, to date, the relationship between PPAR β and TLR9 has not yet been examined.

Mitochondrial homeostasis contains a network formed by continuous fission and fusion events, and an imbalance of these events leads to apoptosis and cell death [54]. During mitochondrial injury, cytochrome c is released from the inner mitochondrial membrane into the cytosol, thereby initiating the intrinsic apoptotic pathway and caspase activation [9]. Cytochrome c, a marker for circulating mitochondrial DNA, was decreased in Tlr9 knock-out mice subjected to severe renal ischemia [13]. Peerapanyasut et al. [29] showed that Drp-1, a regulator for

mitochondrial fission (fragmentation), increases in hepatic tissue after renal IRI. Additionally, mitochondrial fragmentation depletes ATP due to an overproduction of ROS [55]. Consistent with these findings, our data demonstrate that hepatic ATP levels decreased in the IRI-placebo group, which is restored by treprostinil. Proteomic analyses confirmed the hepatic mitochondrial injury by the protein expression patterns of several ATP synthase subunits in IRI-placebo animals, all of which were upregulated by treprostinil. Furthermore, our data show that Drp-1 and cytochrome c protein expression are upregulated in the mitochondria and cytosol, respectively. Moreover, a decrease in procaspase-3 (inactive) and increase in the cleaved (active) forms indicate apoptotic injury [9]. Cleaved-caspase-3 promotes apoptosis by further triggering the apoptotic cascade in the intrinsic apoptotic pathway [9]. In agreement with Lai et al. [10], our study also demonstrates that renal IRI significantly increased hepatic cleaved caspase-3 protein expression, which treprostinil significantly reduced. Altogether, our data indicate that treprostinil restores hepatic ATP and reduces mitochondrial-mediated apoptosis during renal IRI.

Lastly, downregulation of PGC-1 α , a major regulator of mitochondrial biogenesis, decreases mitochondrial content which exacerbates mitochondrial-mediated apoptosis [33]. In this study, treprostinil counteracted renal IRI-induced hepatic mitochondrial injury and restored hepatic *Pgc-1 α* expression and mtDNA copy number. PGC-1 α also regulates mitochondrial antioxidant activity and Sirt3 activity [56]. Deficiencies in Sirt3 promote further oxidative stress by inducing lipid peroxidation and decreasing SOD activity [57], as well as downregulating murine Mfn1 and Mfn2 protein in the brain [58], illustrating the importance of maintaining

hepatic Pgc-1 α and Sirt3 levels. Here, we demonstrate that hepatic Sirt3 protein expression is reduced in the IRI-placebo group as well as *Mfn1* and *Mfn2*.

Collectively, our data demonstrate that treprostinil alleviates hepatic mitochondrial injury by improving mitochondrial dynamics during renal IRI.

In conclusion, there is currently no treatment for liver injury during kidney IRI and patients who develop liver injury following AKI are at a higher risk for multi-organ injury and subsequent mortality. This study demonstrates the hepatoprotective effects of treprostinil during renal IRI *in vivo*. Specifically, the improved hepatic function, restored antioxidant levels, reduced inflammatory response, mitochondrial-mediated apoptosis, and improved mitochondrial dynamics strongly indicate that treprostinil protects the liver during renal IRI by reducing the downstream effects of Tlr9-mediated in liver injury. The hepatic proteome data provide further insight to the protein network and pathways regulated by treprostinil in reducing mitochondrial injury proteins. Combined with its advantageous properties, the findings in this study support the efficacy of treprostinil in reducing hepatic dysfunction during renal IRI and, further, support treprostinil as potential therapy to alleviate hepatic injury during clinical AKI.

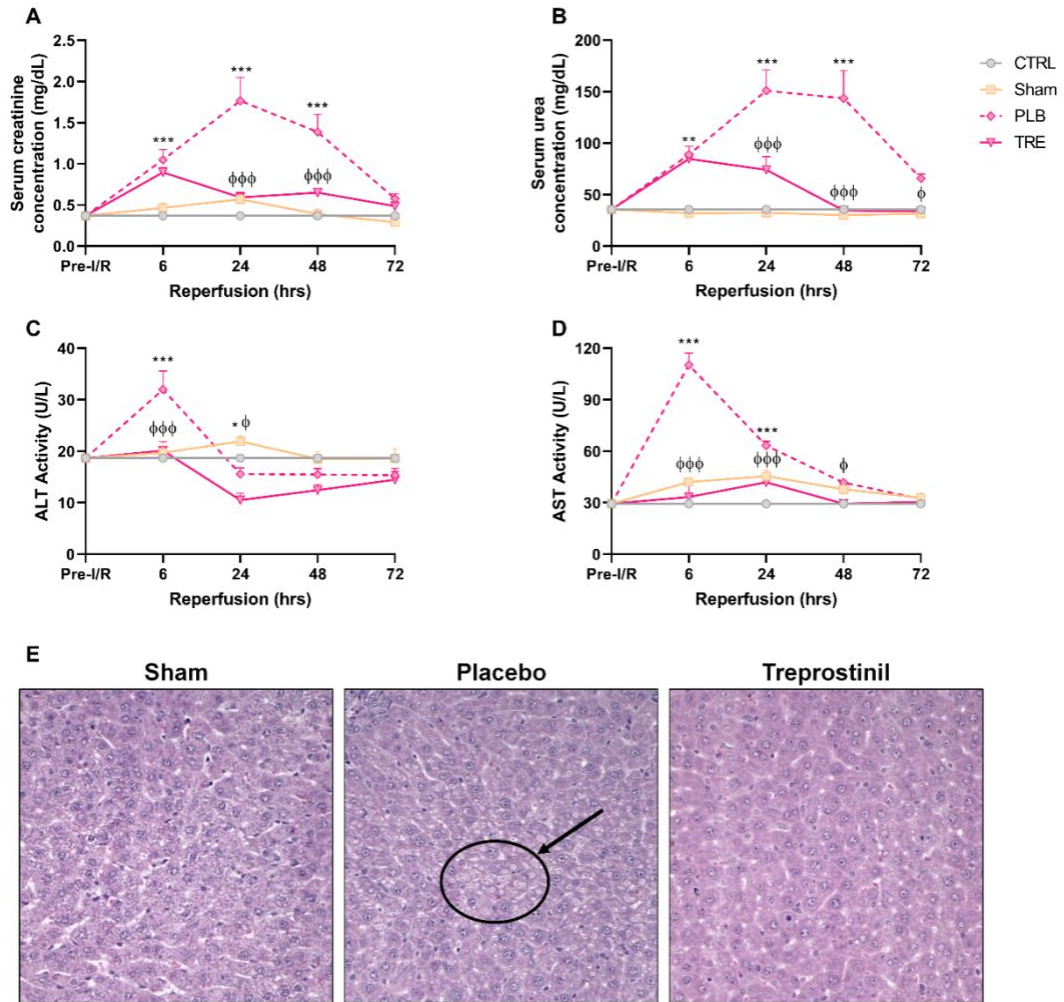


Figure 1. Treprostinil reduces kidney and liver dysfunction. **(A)** SCr, **(B)** BUN, **(C)** ALT, and **(D)** AST measured at pre-IRI (baseline) 1-72 hours post-reperfusion in control-, sham-, placebo-, and treprostinil-treated animals. Data are represented as mean \pm SEM. * $P < 0.05$, ** $P < 0.01$, *** $P < 0.001$ vs. sham; $\phi P < 0.05$, $\phi\phi P < 0.01$, $\phi\phi\phi P < 0.001$ vs. IRI-placebo ($n = 3-10$ /group). Two-way ANOVA, Tukey's multiple comparisons test. **(E)** H&E (hematoxylin & eosin) staining of liver sections obtained from sham-operated, IRI-placebo or IRI-treprostinil rats at 6-hours post-reperfusion. Black circle and arrow indicate increased vacuolation in hepatocytes in IRI-placebo group. Data are representative of 4-5 sections per sample ($n = 4$ /group, $\times 400$). *SCr*: Serum creatinine; *BUN*: Blood urea nitrogen; *ALT*: Alanine aminotransferase; *AST*: aspartate aminotransferase; *CTRL*: Control; *PLB*: Placebo; *TRE*: Treprostinil.

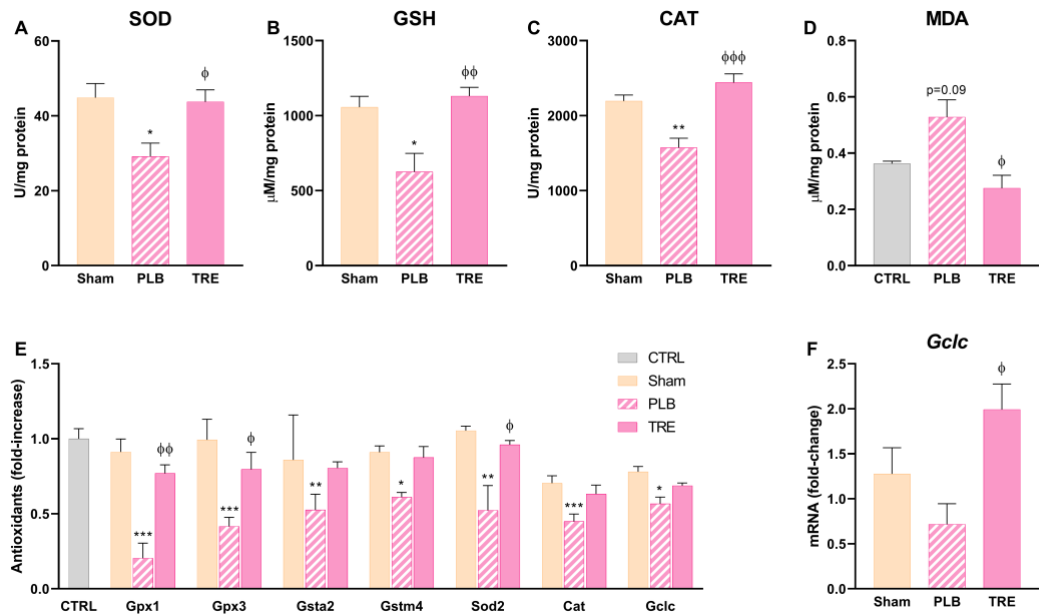


Figure 2. Treprostlinil alleviates hepatic oxidative stress levels. (A) SOD, (B) GSH, and (C) CAT activity levels at 1-, 6-, and 24-hours post-reperfusion; (D) Lipid peroxidation levels at 48-hours post-reperfusion; (E) Antioxidants at 24-hours post-reperfusion measured by SWATH-MS based proteomics normalized to Gapdh and expressed as a fold-change over control. (F) *Gclc* mRNA levels at 48-hours post-reperfusion normalized to *18S*. Data represented are mean ± SEM. *P<0.05, **P<0.01, ***P<0.001 vs. control or sham; φP<0.05, φφP<0.01, φφφP<0.001 vs. IRI-placebo (n = 3-6/group). One- or two-way ANOVA, Tukey's multiple comparisons test. *SOD*: Superoxide dismutase; *GSH*: Glutathione; *CAT*: Catalase; *SWATH-MS*: Sequential windowed acquisition of all theoretical fragment ion mass spectra; *MDA*: Malondialdehyde; *Gpx*: Glutathione peroxidase; *Gsta2*: Glutathione S-transferase alpha 2; *Gstm4*: Glutathione S-transferase mu 4; *Gclc*: Glutamate-cysteine ligase catalytic subunit; *CTRL*: Control; *PLB*: IRI-placebo; *TRE*: IRI-treprostlinil.

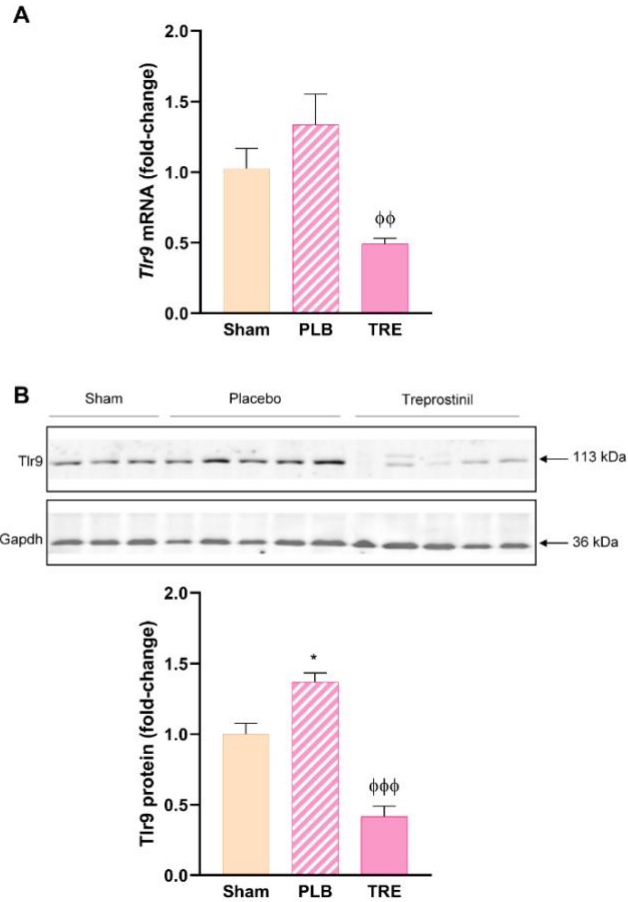


Figure 3. Treprostiniil reduces hepatic Tlr9 mRNA and protein expression. **(A)** *Tlr9* at 48-hours post-reperfusion was measured by qPCR, normalized to *18S*, and expressed as fold-change over sham. **(B)** Tlr9 at 48-hours post-reperfusion was measured by western blot normalized to Gapdh, and quantification was performed using Image J software; Data are represented as mean \pm SEM. * $P < 0.05$ vs. sham; $\phi\phi P < 0.01$, $\phi\phi\phi P < 0.001$ vs. IRI-placebo (n = 3-5/group). One-way ANOVA, Tukey's multiple comparisons test. *Tlr9*: Toll-like receptor 9; *Gapdh*: Glyceraldehyde 3-phosphate dehydrogenase; *PLB*: IRI-placebo; *TRE*: IRI-treprostiniil.

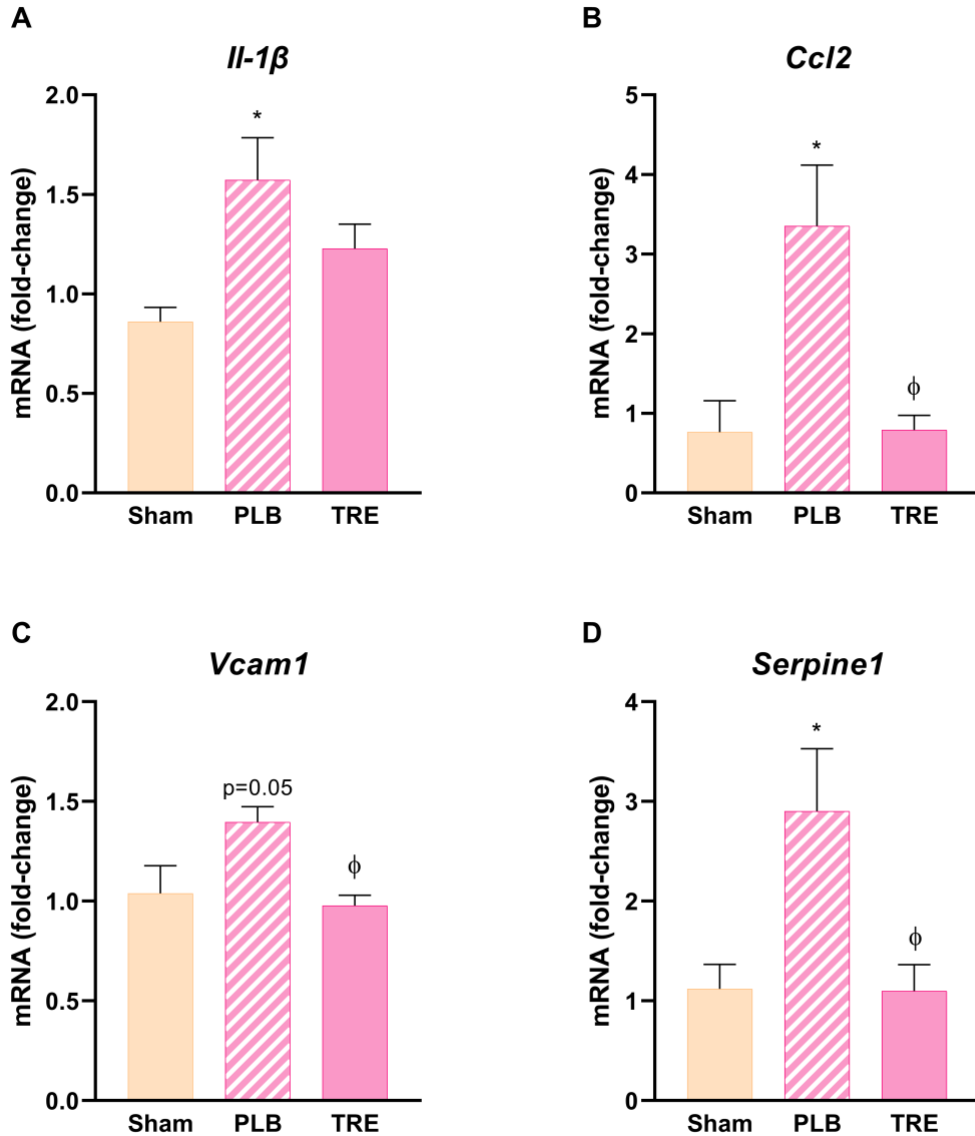


Figure 4. Treprostnil reduces hepatic inflammation. (A) *Il-1 β* at 6-hours post-reperfusion, (B) *Ccl2* at 6-hours post-reperfusion, (C) *Vcam1* at 24-hours post-reperfusion, and (D) *Serpine1* at 24-hours post-reperfusion were measured by qPCR, normalized to *18S*, and expressed as a fold-increase over sham. Data are represented as mean \pm SEM. * $P < 0.05$ vs. sham; $\phi P < 0.05$ vs. IRI-placebo (n = 4-5/group). One-way ANOVA, Tukey's multiple comparisons test. *Il-1 β* : Interleukin-1 beta; *Ccl2*: Chemokine ligand 2; *Vcam1*: Vascular cell adhesion molecule 1; *Serpine1*: Serine protease inhibitor, family E, member 1; PLB: IRI-placebo; TRE: IRI-treprostnil.

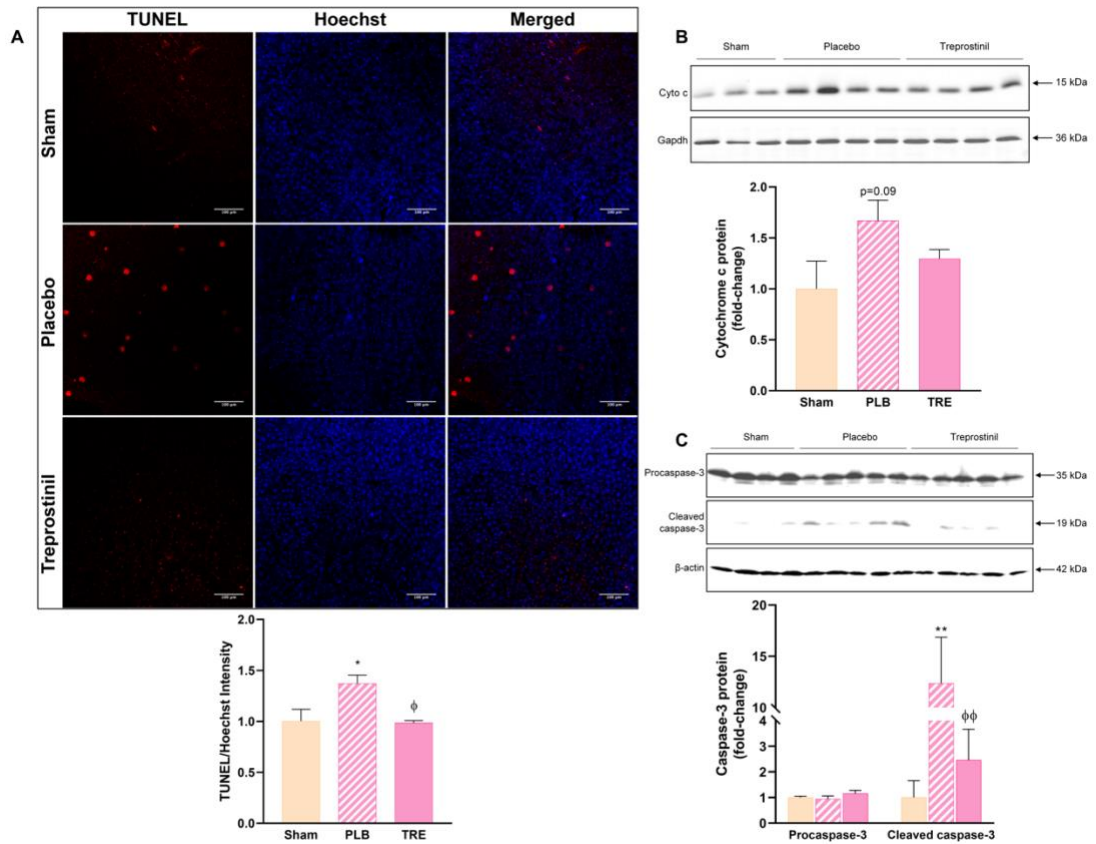


Figure 5. Treprostsinil inhibits hepatic apoptosis. **(A)** Hepatic apoptosis *in situ*, measured by TUNEL staining (red fluorescence) in rat liver sections at 6-hours post-reperfusion ($\times 200$, scale bar = 100 μm). Nuclei were counterstained with Hoechst (blue fluorescence). **(B)** Hepatic cytochrome c protein levels at 3-hours post-reperfusion measured by western blot, normalized to Gapdh; **(C)** Cleaved (activated) caspase-3 protein levels at 48-hours post-reperfusion measured by western blot, normalized to β -actin, and quantified using Image J software. Data are represented as mean \pm SEM. * $P < 0.05$, ** $P < 0.01$ vs. sham; $\phi P < 0.05$, $\phi\phi P < 0.01$ vs. IRI-placebo ($n = 3-5/\text{group}$). One-way ANOVA, Tukey's multiple comparisons test. *TUNEL*: Terminal deoxynucleotidyl transferase dUTP nick end labeling; *Cyto c*: cytochrome c; *Gapdh*: Glyceraldehyde 3-phosphate dehydrogenase; *PLB*: IRI-placebo; *TRE*: IRI-treprostsinil.

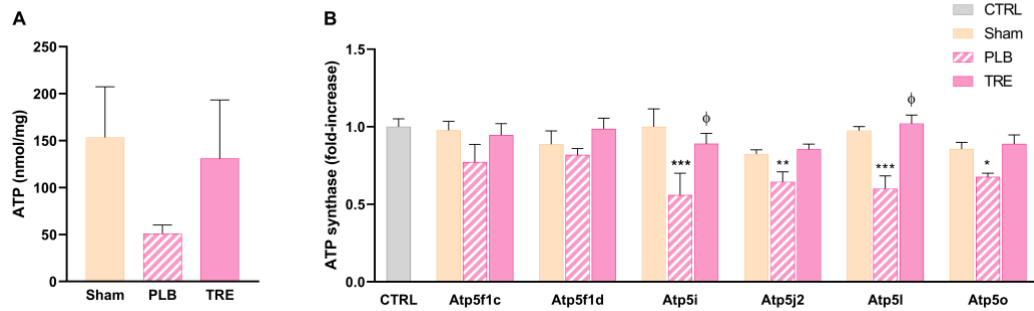


Figure 6. Treprostini restores hepatic ATP and ATP synthase levels. **(A)** Hepatic ATP levels at 6-hours post-reperfusion measured by bioluminescent assay; **(B)** ATP synthase subunits at 24-hours post-reperfusion measured by SWATH-MS based proteomics, normalized to Gapdh, and expressed as fold-change over control. Data represented are mean \pm SEM. * $P < 0.05$, ** $P < 0.01$, *** $P < 0.001$ vs. sham; $\phi P < 0.05$ vs. IRI-placebo (n = 4-6/group). One- or two-way ANOVA, Tukey's multiple comparisons test. ATP: Adenosine triphosphate; SWATH-MS: *Sequential windowed acquisition of all theoretical fragment ion mass spectra*; Atp5f1c: ATP synthase F1 subunit gamma; Atp5f1d: ATP synthase F1 subunit delta; Atp5i: ATP synthase subunit e; Atp5j2: ATP synthase subunit f; Atp5l: ATP synthase subunit g; Atp5o: ATP synthase subunit o; CTRL: Control; PLB: IRI-placebo; TRE: IRI-treprostini.

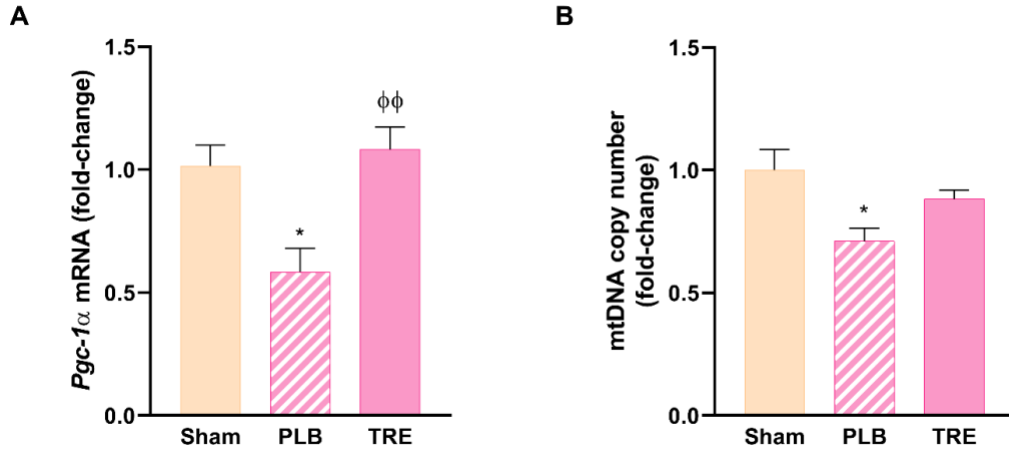


Figure 7. Treprostiniil preserves mitochondrial biogenesis and mtDNA. **(A)** Hepatic mRNA expression of *Pgc-1 α* at 24-hours post-reperfusion was measured by qPCR, normalized to *18S* and is expressed as a fold-change over sham. **(B)** Hepatic mtDNA copy number at 6-hours post-reperfusion, measured by real-time qPCR; Data are represented as mean \pm SEM. * $P < 0.05$ vs. sham; $\phi\phi P < 0.01$ vs. IRI-placebo (n = 4-5/group). One-way ANOVA, Tukey's multiple comparisons test. *Pgc-1*: Peroxisome proliferator-activated receptor gamma coactivator 1 alpha; mtDNA: mitochondrial DNA; PLB: IRI-placebo; TRE: IRI-treprostiniil.

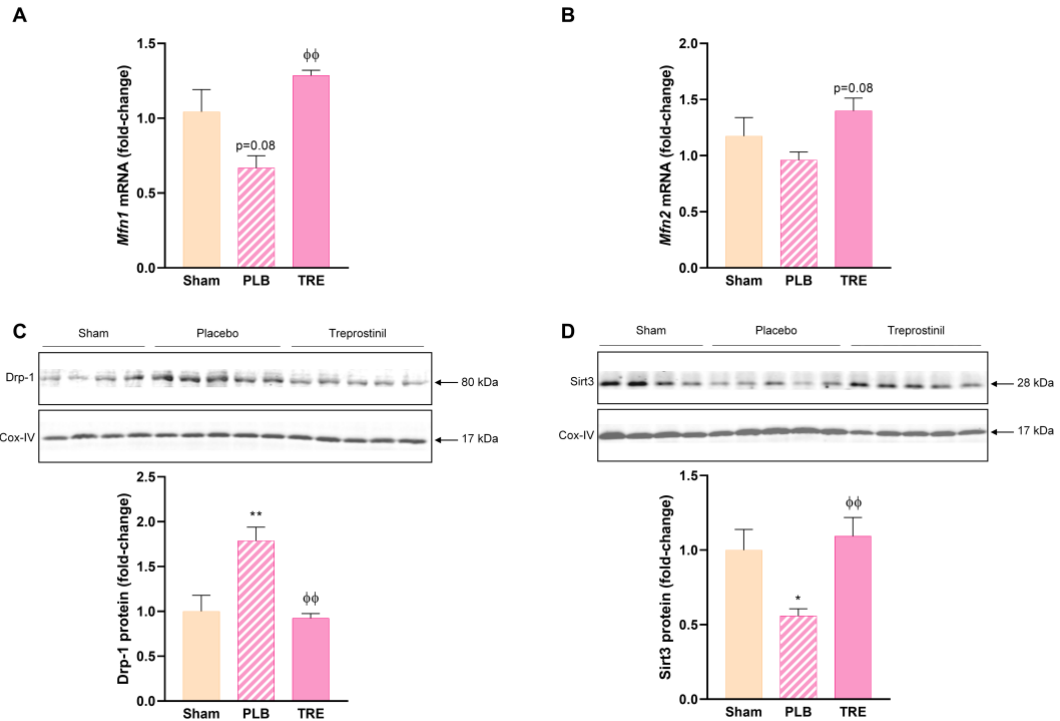


Figure 8. Treprostinil improves hepatic mitochondrial dynamics after renal IRI. Hepatic mRNA expressions of (A) *Mfn1* and (B) *Mfn2* at 24-hours post-reperfusion measured by qPCR, normalized to *18S* and expressed as fold-change over sham. Hepatic protein expression of (C) Drp-1 and (D) Sirt3 at 3- and 6-hr post-reperfusion, respectively measured by western blot, normalized to Cox-IV and quantified using Image J software. Data represented are mean \pm SEM. *P<0.05, **P<0.01 vs. sham; $\phi\phi$ P<0.01 vs. IRI-placebo (n = 4-5/group). One-way ANOVA, Tukey's multiple comparisons test. *Mfn1*: Mitofusin-1; *Mfn2*: Mitofusin-2; *Drp-1*: Dynamin-related protein 1; *Sirt3*: NAD-dependent deacetylase sirtuin-3; *Cox-IV*: Cytochrome c oxidase subunit 4; PLB: IRI-placebo; TRE: IRI-treprostinil.

REFERENCES

- [1] S.F. Smith, S.A. Hosgood, M.L. Nicholson, Ischemia-reperfusion injury in renal transplantation: 3 key signaling pathways in tubular epithelial cells, *Kidney Int* 95(1) (2019) 50-56.
- [2] S. Elshazly, E. Soliman, PPAR gamma agonist, pioglitazone, rescues liver damage induced by renal ischemia/reperfusion injury, *Toxicol Appl Pharmacol* 362 (2019) 86-94.
- [3] S.A. Lee, M. Cozzi, E.L. Bush, H. Rabb, Distant Organ Dysfunction in Acute Kidney Injury: A Review, *Am J Kidney Dis* 72(6) (2018) 846-856.
- [4] A.S. Awad, R. Kamel, M.A. Sherief, Effect of thymoquinone on hepatorenal dysfunction and alteration of CYP3A1 and spermidine/spermine N-1-acetyltransferase gene expression induced by renal ischaemia-reperfusion in rats, *J Pharm Pharmacol* 63(8) (2011) 1037-42.
- [5] M.M. Farag, A.A. Khalifa, W.F. Elhadidy, R.M. Rashad, Hepatorenal protection in renal ischemia/reperfusion by celecoxib and pentoxifylline, *J Surg Res* 204(1) (2016) 183-91.
- [6] Y. Shang, Y.L. Siow, C.K. Isaak, K. O, Downregulation of Glutathione Biosynthesis Contributes to Oxidative Stress and Liver Dysfunction in Acute Kidney Injury, *Oxid Med Cell Longev* 2016 (2016) 9707292.
- [7] F. Gholampour, Z. Sadidi, Hepatorenal protection during renal ischemia by quercetin and remote ischemic preconditioning, *J Surg Res* 231 (2018) 224-233.
- [8] S.H. Kim, H. Kim, Inhibitory Effect of Astaxanthin on Oxidative Stress-Induced Mitochondrial Dysfunction-A Mini-Review, *Nutrients* 10(9) (2018).

- [9] Y.P. Ow, D.R. Green, Z. Hao, T.W. Mak, Cytochrome c: functions beyond respiration, *Nat Rev Mol Cell Biol* 9(7) (2008) 532-42.
- [10] Y. Lai, J. Deng, M. Wang, M. Wang, L. Zhou, G. Meng, Z. Zhou, Y. Wang, F. Guo, M. Yin, X. Zhou, H. Jiang, Vagus nerve stimulation protects against acute liver injury induced by renal ischemia reperfusion via antioxidant stress and anti-inflammation, *Biomed Pharmacother* 117 (2019) 109062.
- [11] F. Golab, M. Kadkhodae, M. Zahmatkesh, M. Hedayati, H. Arab, R. Schuster, K. Zahedi, A.B. Lentsch, M. Soleimani, Ischemic and non-ischemic acute kidney injury cause hepatic damage, *Kidney Int* 75(8) (2009) 783-92.
- [12] H.J. Anders, Toll-like receptors and danger signaling in kidney injury, *J Am Soc Nephrol* 21(8) (2010) 1270-4.
- [13] P.J. Bakker, A.M. Scantlebery, L.M. Butter, N. Claessen, G.J. Teske, T. van der Poll, S. Florquin, J.C. Leemans, TLR9 Mediates Remote Liver Injury following Severe Renal Ischemia Reperfusion, *PLoS One* 10(9) (2015) e0137511.
- [14] B. Gao, Innate immunity and steatohepatitis: a critical role of another toll (TLR-9), *Gastroenterology* 139(1) (2010) 27-30.
- [15] A.W. El-Hattab, W.J. Craigen, F. Scaglia, Mitochondrial DNA maintenance defects, *Biochim Biophys Acta Mol Basis Dis* 1863(6) (2017) 1539-1555.
- [16] R. Yu, U. Lendahl, M. Nister, J. Zhao, Regulation of Mammalian Mitochondrial Dynamics: Opportunities and Challenges, *Front Endocrinol (Lausanne)* 11 (2020) 374.
- [17] T. Dusabimana, S.R. Kim, H.J. Kim, S.W. Park, H. Kim, Nobiletin ameliorates hepatic ischemia and reperfusion injury through the activation of SIRT-1/FOXO3a-mediated autophagy and mitochondrial biogenesis, *Exp Mol Med* 51(4) (2019) 1-16.

- [18] Q. Zhang, M. Raouf, Y. Chen, Y. Sumi, T. Sursal, W. Junger, K. Brohi, K. Itagaki, C.J. Hauser, Circulating mitochondrial DAMPs cause inflammatory responses to injury, *Nature* 464(7285) (2010) 104-7.
- [19] Y. Zheng, Y. Zhang, Y. Zheng, N. Zhang, Carnosol protects against renal ischemia-reperfusion injury in rats, *Exp Anim* 67(4) (2018) 545-553.
- [20] S.L. Dorris, R.S. Peebles, Jr., PGI₂ as a regulator of inflammatory diseases, *Mediators Inflamm* 2012 (2012) 926968.
- [21] M. Lindegaard Pedersen, M. Kruger, D. Grimm, M. Infanger, M. Wehland, The prostacyclin analogue treprostinil in the treatment of pulmonary arterial hypertension, *Basic Clin Pharmacol Toxicol* (2019).
- [22] T.E. Ding M, Birkenbach M, Gohh R, Akhlaghi F, and Ghonem NS., Treprostinil, a prostacyclin analog, ameliorates renal ischemia-reperfusion injury: Preclinical studies in a rat model of acute kidney injury, *Nephrol Dial Transp.* (2020).
- [23] N. Ghonem, J. Yoshida, N. Murase, S.C. Strom, R. Venkataramanan, Treprostinil Improves Hepatic Cytochrome P450 Activity during Rat Liver Transplantation, *J Clin Exp Hepatol* 2(4) (2012) 323-32.
- [24] P.M. Quiros, A. Goyal, P. Jha, J. Auwerx, Analysis of mtDNA/nDNA Ratio in Mice, *Curr Protoc Mouse Biol* 7(1) (2017) 47-54.
- [25] R. Jamwal, B.J. Barlock, S. Adusumalli, K. Ogasawara, B.L. Simons, F. Akhlaghi, Multiplex and Label-Free Relative Quantification Approach for Studying Protein Abundance of Drug Metabolizing Enzymes in Human Liver Microsomes Using SWATH-MS, *J Proteome Res* 16(11) (2017) 4134-4143.

- [26] M. Kim, S.W. Park, M. Kim, V.D. D'Agati, H.T. Lee, Isoflurane activates intestinal sphingosine kinase to protect against renal ischemia-reperfusion-induced liver and intestine injury, *Anesthesiology* 114(2) (2011) 363-73.
- [27] W. Zou, R.A. Roth, H.S. Younis, E. Malle, P.E. Ganey, Neutrophil-cytokine interactions in a rat model of sulindac-induced idiosyncratic liver injury, *Toxicology* 290(2-3) (2011) 278-85.
- [28] R. Volpes, J.J. Van Den Oord, V.J. Desmet, Vascular adhesion molecules in acute and chronic liver inflammation, *Hepatology* 15(2) (1992) 269-75.
- [29] W. Peerapanyasut, A. Kobroob, S. Palee, N. Chattipakorn, O. Wongmekiat, Activation of Sirtuin 3 and Maintenance of Mitochondrial Integrity by N-Acetylcysteine Protects Against Bisphenol A-Induced Kidney and Liver Toxicity in Rats, *Int J Mol Sci* 20(2) (2019).
- [30] P. Mishra, D.C. Chan, Metabolic regulation of mitochondrial dynamics, *J Cell Biol* 212(4) (2016) 379-87.
- [31] A. Ramachandran, Umbaugh, D.S., Jaeschke, H., Mitochondrial Dynamics in Drug-Induced Liver Injury, *Livers* 1(3) (2021) 102-115.
- [32] B.L. Tang, Sirt1 and the Mitochondria, *Mol Cells* 39(2) (2016) 87-95.
- [33] J. Bi, J. Zhang, Y. Ren, Z. Du, Q. Li, Y. Wang, S. Wei, L. Yang, J. Zhang, C. Liu, Y. Lv, R. Wu, Irisin alleviates liver ischemia-reperfusion injury by inhibiting excessive mitochondrial fission, promoting mitochondrial biogenesis and decreasing oxidative stress, *Redox Biol* 20 (2019) 296-306.

- [34] N. Li, H. Wang, C. Jiang, M. Zhang, Renal ischemia/reperfusion-induced mitophagy protects against renal dysfunction via Drp1-dependent-pathway, *Exp Cell Res* 369(1) (2018) 27-33.
- [35] S.W. Park, S.W. Chen, M. Kim, K.M. Brown, J.K. Kolls, V.D. D'Agati, H.T. Lee, Cytokines induce small intestine and liver injury after renal ischemia or nephrectomy, *Lab Invest* 91(1) (2011) 63-84.
- [36] N. Ghonem, J. Yoshida, D.B. Stolz, A. Humar, T.E. Starzl, N. Murase, R. Venkataramanan, Treprostinil, a prostacyclin analog, ameliorates ischemia-reperfusion injury in rat orthotopic liver transplantation, *Am J Transplant* 11(11) (2011) 2508-16.
- [37] O.A. Almazroo, M.K. Miah, V.C. Pillai, I.H. Shaik, R. Xu, S. Dharmayan, H.J. Johnson, S. Ganesh, R.M. Planinsic, A.J. Demetris, A. Al-Khafaji, R. Lopez, M. Molinari, A.D. Tevar, C. Hughes, A. Humar, R. Venkataramanan, An evaluation of the safety and preliminary efficacy of peri- and post-operative treprostinil in preventing ischemia and reperfusion injury in adult orthotopic liver transplant recipients, *Clin Transplant* 35(6) (2021) e14298.
- [38] K. Lane, J.J. Dixon, I.A. MacPhee, B.J. Philips, Renohepatic crosstalk: does acute kidney injury cause liver dysfunction?, *Nephrol Dial Transplant* 28(7) (2013) 1634-47.
- [39] M. Mohammadi, H. Najafi, Z. Mohamadi Yarijani, G. Vaezi, V. Hojati, Piperine pretreatment attenuates renal ischemia-reperfusion induced liver injury, *Heliyon* 5(8) (2019) e02180.
- [40] J. Deng, J. Feng, T. Liu, X. Lu, W. Wang, N. Liu, Y. Lv, Q. Liu, C. Guo, Y. Zhou, Beraprost sodium preconditioning prevents inflammation, apoptosis, and

autophagy during hepatic ischemia-reperfusion injury in mice via the P38 and JNK pathways, *Drug Des Devel Ther* 12 (2018) 4067-4082.

[41] C. O'Connell, D. Amar, A. Boucly, L. Savale, X. Jais, M.C. Chaumais, D. Montani, M. Humbert, G. Simonneau, O. Sitbon, Comparative Safety and Tolerability of Prostacyclins in Pulmonary Hypertension, *Drug Saf* 39(4) (2016) 287-94.

[42] M. Serteser, T. Koken, A. Kahraman, K. Yilmaz, G. Akbulut, O.N. Dilek, Changes in hepatic TNF-alpha levels, antioxidant status, and oxidation products after renal ischemia/reperfusion injury in mice, *J Surg Res* 107(2) (2002) 234-40.

[43] M. Zhu, A.S. Barbas, L. Lin, U. Scheuermann, M. Bishawi, T.V. Brennan, Mitochondria Released by Apoptotic Cell Death Initiate Innate Immune Responses, *Immunohorizons* 2(11) (2018) 384-397.

[44] Z.M. Bamboat, V.P. Balachandran, L.M. Ocuin, H. Obaid, G. Plitas, R.P. DeMatteo, Toll-like receptor 9 inhibition confers protection from liver ischemia-reperfusion injury, *Hepatology* 51(2) (2010) 621-32.

[45] A. Taki-Eldin, L. Zhou, H.Y. Xie, K.J. Chen, D. Yu, Y. He, S.S. Zheng, Triiodothyronine attenuates hepatic ischemia/reperfusion injury in a partial hepatectomy model through inhibition of proinflammatory cytokines, transcription factors, and adhesion molecules, *J Surg Res* 178(2) (2012) 646-56.

[46] G. Lassailly, M. Bou Saleh, N. Leleu-Chavain, M. Ningarhari, E. Gantier, R. Carpentier, F. Artru, V. Gnemmi, B. Bertin, P. Maboudou, D. Betbeder, C. Gheeraert, F. Maggiotto, S. Dharancy, P. Mathurin, A. Louvet, L. Dubuquoy, Nucleotide-binding oligomerization domain 1 (NOD1) modulates liver ischemia reperfusion through the expression adhesion molecules, *J Hepatol* 70(6) (2019) 1159-1169.

- [47] D.E. Vaughan, PAI-1 and atherothrombosis, *J Thromb Haemost* 3(8) (2005) 1879-83.
- [48] H.H. Chen, T.W. Chen, H. Lin, Prostacyclin-induced peroxisome proliferator-activated receptor-alpha translocation attenuates NF-kappaB and TNF-alpha activation after renal ischemia-reperfusion injury, *Am J Physiol Renal Physiol* 297(4) (2009) F1109-18.
- [49] S. Fan, X. Huang, S. Wang, C. Li, Z. Zhang, M. Xie, S. Nie, Combinatorial usage of fungal polysaccharides from *Cordyceps sinensis* and *Ganoderma atrum* ameliorate drug-induced liver injury in mice, *Food Chem Toxicol* 119 (2018) 66-72.
- [50] F.Y. Ali, S.J. Davidson, L.A. Moraes, S.L. Traves, M. Paul-Clark, D. Bishop-Bailey, T.D. Warner, J.A. Mitchell, Role of nuclear receptor signaling in platelets: antithrombotic effects of PPARbeta, *FASEB J* 20(2) (2006) 326-8.
- [51] Y. Wang, T. Nakajima, F.J. Gonzalez, N. Tanaka, PPARs as Metabolic Regulators in the Liver: Lessons from Liver-Specific PPAR-Null Mice, *Int J Mol Sci* 21(6) (2020).
- [52] M. Zarei, D. Aguilar-Recarte, X. Palomer, M. Vazquez-Carrera, Revealing the role of peroxisome proliferator-activated receptor beta/delta in nonalcoholic fatty liver disease, *Metabolism* 114 (2021) 154342.
- [53] N. Dana, G. Vaseghi, S. Haghjooy Javanmard, Crosstalk between Peroxisome Proliferator-Activated Receptors and Toll-Like Receptors: A Systematic Review, *Adv Pharm Bull* 9(1) (2019) 12-21.

- [54] V. Carelli, A. Maresca, L. Caporali, S. Trifunov, C. Zanna, M. Rugolo, Mitochondria: Biogenesis and mitophagy balance in segregation and clonal expansion of mitochondrial DNA mutations, *Int J Biochem Cell Biol* 63 (2015) 21-4.
- [55] M. Hasnat, Z. Yuan, A. Ullah, M. Naveed, F. Raza, M. Baig, A. Khan, D. Xu, Y. Su, L. Sun, L. Zhang, Z. Jiang, Mitochondria-dependent apoptosis in triptolide-induced hepatotoxicity is associated with the Drp1 activation, *Toxicol Mech Methods* 30(2) (2020) 124-133.
- [56] S. Rius-Perez, I. Torres-Cuevas, I. Millan, A.L. Ortega, S. Perez, PGC-1alpha, Inflammation, and Oxidative Stress: An Integrative View in Metabolism, *Oxid Med Cell Longev* 2020 (2020) 1452696.
- [57] X. Li, S. Song, M. Xu, Y. Hua, Y. Ding, X. Shan, G. Meng, Y. Wang, Sirtuin3 deficiency exacerbates carbon tetrachloride-induced hepatic injury in mice, *J Biochem Mol Toxicol* 33(2) (2019) e22249.
- [58] A. Tyagi, C.U. Nguyen, T. Chong, C.R. Michel, K.S. Fritz, N. Reisdorph, L. Knaub, J.E.B. Reusch, S. Pugazhenti, SIRT3 deficiency-induced mitochondrial dysfunction and inflammasome formation in the brain, *Sci Rep* 8(1) (2018) 17547.